Int J Clin Exp Pathol 2015;8(10):12284-12291
www.ijcep.com /ISSN:1936-2625/IJCEP0014765

Original Article

Pathologic changes of wound tissue in rats with stage III pressure ulcers treated by transplantation of human amniotic epithelial cells

Xilan Zheng[1], Zhixia Jiang[1], Aiting Zhou[1], Limei Yu[2], Mingtao Quan[3], Huagang Cheng[4]

[1]Nursing College, Zunyi Medical College, Zunyi 563000, Guizhou, China; [2]Cell Engineering Laboratory, The Affiliated Hospital of Zunyi Medical College, Zunyi 563000, Guizhou, China; [3]Intensive Care Unit (ICU), The Affiliated Hospital of Zunyi Medical College, Zunyi 563000, Guizhou, China; [4]Clinical School, The Affiliated Hospital of Zunyi Medical College, Zunyi 563000, Guizhou, China

Received August 19, 2015; Accepted September 24, 2015; Epub October 1, 2015; Published October 15, 2015

Abstract: This study aims to determine the impact of orthotopic transplantation of human amniotic epithelial cells (hAECs) on the pathologic changes of wound tissues in a self-prepared rat stage III pressure ulcer model. Ninety-six SD rats were randomly divided into the model group (group M), hAEC transplantation group (group H), traditional treatment group (group T), and the control group (group C), with 24 rats in each group. The wound healing time was observed in 6 rats from each group, and 6 rats of each group were selected for post-modeling on day(s) (D) 1, 3, and 7 for HE staining to compare the pathological changes. The healing time of group H was significantly shorter than the other three groups. Moreover, pathological observations revealed that group H exhibited significant proliferation of fibrous tissues and vessels in the dermal layer, and the appearance time and degree of skin appendages were significantly greater than that observed in the other three groups. Pathological observations showed that hAEC transplantation could significantly speed up the healing of stage III pressure ulcer.

Keywords: Human amniotic epithelial cells, stage III pressure ulcer, pathology

Introduction

Pressure ulcer (PU) is localized injury to the skin and/or underlying tissue usually over a bony prominence, as a result of pressure, or pressure in combination with shear. A number of contributing or confounding factors are also associated with pressure ulcers; the significance of these factors is yet to be elucidated [1]. PU normally has a large damage range, easily causing sepsis, systemic failure, and other life-threatening complications. Moreover, PU would not only cause patients a considerable amount of pain, but also increase body's consumption, thus affecting the recovery of primary diseases and increasing the overall cost of health care [2]. In recent years, developments in stem cell technology have provided new directions for the treatments of a variety of refractory diseases [3]. In this study, we used Sprague-Dawley (SD) rats to generate a stage III PU model and transplanted human amniotic epithelial cells (hAECs) to treat stage III PU, aiming to evaluate its impacts on healing time and pathological conditions of PU and providing a basis for preclinical studies of hAECs in treating refractory stage III PU.

Materials and methods

Animals and grouping

Ninety-six adult male Sprague-Dawley (SD) rats, weighing between 120 and 150 g, were purchased from the Chongqing Tengxin Bill animals Sales Co., Ltd. [License No: SCXK (Yu) 2012-0005], and divided randomly into groups M, T, H, and C, with 24 rats in each group. In group M, the wound was protected by replacing the medical sterile applicator daily [4]. Group T was disinfected with 0.5% povidone-iodine solution, and the wound was then exposed to infrared irradiation for 15-20 min once per day [5]. The wound was then covered with 0.5% povidone-iodine-

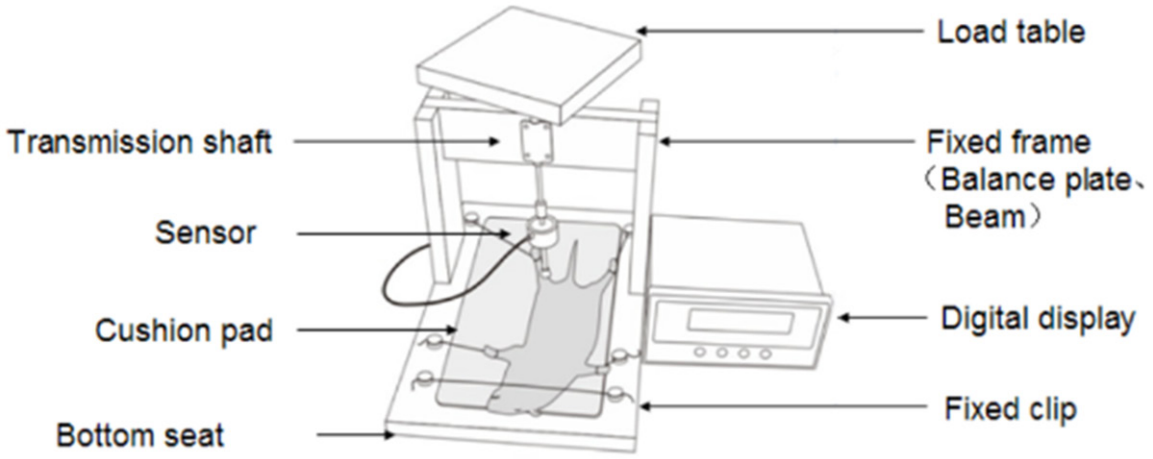

Figure 1. Working line chart of animal pressure ulcer model machine (China patent, No. 201420090436x).

soaked gauze, and fixed the gauze with the medical sterile applicator, and sterilized. The povidone-iodine gauze was replaced daily and the wound was disinfected under aseptic conditions and exposed to infrared irradiation [6]. Group H was immediately subcutaneously injected with normal saline-suspended ~4th-5th generation hAECs (5×10^5 cells/rat), and the wound was protected with a medical sterile applicator, which was replaced daily. In group C rats, the legs were shaved, anesthetized, and fixed onto an operating table at the same time as other groups, while did not modeling and treatment. Animals and operating procedures used in this study were compliant with the relevant ethical requirements for animal studies.

Acquisition, culture, and identification of hAECs

Amniotic membranes were obtained from the parturients at the affiliated Hospital of Zunyi Medical College after obtaining their informed consent. The amniotic membrane was peeled from the fresh placenta of a full-term parturient on whom C-section was performed, prior to which physical examinations were carried out to exclude the possibility of hepatitis B, hepatitis C, syphilis, human immunodeficiency virus (HIV), and other diseases [7]. Peeled amniotic membranes were cultured from fresh placenta under aseptic conditions. Membranes were rinsed with freshly prepared D-Hank's solution before the experiment and then cut into pieces. Next, 0.02% ethylene diamine tetraacetic acid (EDTA)-containing 0.05% trypsin solution (for digestion) followed by addition of 10% Fetal Bovine Serum (FBS)-containing medium to terminate digestion [8]. The cell precipitate was then resuspended in L-DMEM, containing 1% β-mercaptoethanol, 1% GlutaMAX, 10% FBS, 10 μg/mL EGF, and 1% NEAA. The above cultured cells were namely the primary hAECs [9]. The isolated primary cells were then seeded in 25 cm^2 flasks [10] with a density of 5×10^5 cells/mL for 72-96 h of culture. Once the cells exhibited >80% confluence, a solution of 0.125% trypsin and 0.02% EDTA was added for digestion and subculture [11]. Flow cytometery and immunocytochemistry were then carried out to identify hAECs [12].

Model preparation

Based on a previously reported method [13], rats were fixed in the supine position onto a cushion pad for anesthesia with propofol (the first anesthesia dose, 10 $mg\cdot kg^{-1}$ with a 30 $mg\cdot kg^{-1}\cdot h^{-1}$ maintenance dose; the second anesthesia dose, 8 $mg\cdot kg^{-1}$ with a 20 $mg\cdot kg^{-1}\cdot h^{-1}$ maintenance dose). We used a self-made PU preparing apparatus (**Figure 1**), after anesthetization and fixed the rat, interior skin, and muscle tissues of the left thigh were placed under the transmission shaft. Sandbags were then placed onto the load table such that the local tissues would be under pressure, followed by ischemic necrosis [8]. The modeling site was compressed for 2 h, and reperfusion was then performed for 0.5 h, 3 times a day for 7 consecutive days.

Transplantation of hAECs

The P4 hAECs digested in the single cell suspension, adjusted to a cell density of 1×10^6

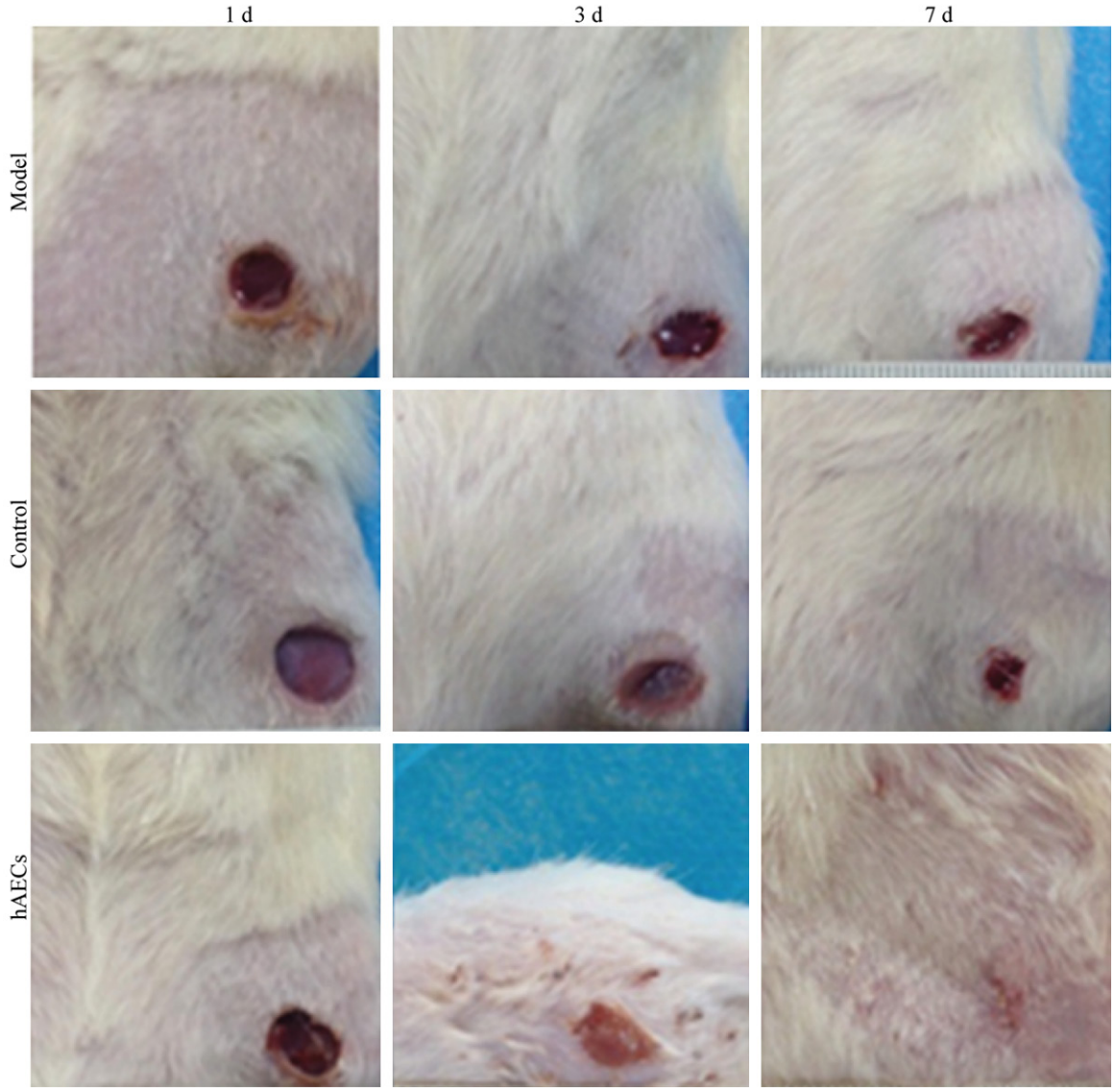

Figure 2. Wound healing comparison among the groups on D1, 3 and 7.

cells/960 μL with D-PBS. The cell suspension (480 μL) was subcutaneously injected in each rat and the wound center was demarcated with a circle, and the greatest distance from the center was considered the radius for drawing a circle. A concentric circle with the half the radius of the original circle was drawn, following which 4 straight lines were drawn through the center, dividing the two circles into eight sectors. The 45° extension cord intersected the two circles and formed eight points, such that a total of 16 transplantation points could be obtained. One 50 μL micro syringe was then used to inject 30 μL of the cell suspension into each transplantation point.

Detection of wound healing rate and healing time

One disposable, sterile, transparent sheet of graph paper was used to draw the shape of the wound for calculating the wound area and the wound healing rate. Wound healing rate = (original wound area - area when detected)/original wound area ×100%, when the healing rate was more than 95%, it could be considered as completely cured [9].

The transparent graph paper was then cut in into 5×5 cm^2 fragments and sterilized with ethylene oxide. Then shape of the wound was then drawn on the transparent graph paper. When

Table 1. Changes of wound healing rates of skin and muscle tissues among groups after hAECs transplantation (%) ($\bar{x} \pm s$, n=6)

Group	D1	D3	D7 d
M	9.67±1.11	14.83±1.47	70.29±2.54
T	10.17±1.17*	16.33±1.11	71.71±3.45*
H	12.33±1.97*,Δ	47.67±3.14*,Δ	91.43±2.13*,Δ

Compared with group M, *P<0.01; compared with group T, ΔP<0.05.

Table 2. Comparison of wound healing time ($\bar{x} \pm s$, n=6)

Group	Healing time (d)
M	9.83±0.69**
T	9.17±0.69*,#
H	5.5±1.52

Compared with group H, *P<0.05, **P<0.01; Compared with group M, #P<0.05.

the pattern filled a large lattice, it was counted as 1 cm^2, and when it filled a small lattice, it was counted as 0.01 cm^2, if the pattern could not fill a small lattice, it was counted in accordance with the rounding-off method. Greater than half the lattice was counted as 0.01 cm^2, while smaller than half the lattice was not counted. Repeated measurements were performed to reduce the error to less than 0.01 cm^2, which fell within the allowable range for this experiment.

Histopathological examination

Six rats from each group were randomly selected and treated by cervical dislocation method on the post-hAEC transplantation day(s) (D) 1, 3 and 7, then 1 cm^2 of wound central tissues was taken, soaked in 10-fold 4% paraformaldehyde solution for 24 h of fixation. The specimens were then sent to the department of Pathology at the Affiliated Hospital of Zunyi Medical College, for paraffin embedding, slicing, hematoxylin-eosin (HE) staining, and histopathological examination.

Statistical analysis

The experimental data were expressed as mean ± standard deviation ($\bar{x} \pm s$), SPSS19.0 software was used for statistical analysis, and ANOVA was used for the intergroup comparison, with P<0.05 considered statistically significant.

Results

Wound observations

Figure 2 shows that, on D1 of treatment, group M secreted a yellow, purulent fluid in the wound. Groups T and H secreted a pale yellow transparent exudate. On D3 of treatment, group T showed no wound exudate, group M showed a small amount of yellow exudate, while group H exhibited crusting on skin surface without an exudate. On D7 of treatment, group M showed no crusting on the skin surface, with a yellow transparent exudate, group T exhibited crusting on partial skin surface with no significant exudate, group H showed a healed wound, and group T showed a partially healed wound, and the wound area in group T was smaller than group M.

Changes in wound healing rates of skin and muscle tissues

As shown in **Table 1**, on D1 of treatment, the wound healing rates of group T and group H were higher than group M (P<0.05). On D3, the wound healing rate of group H was significantly higher than group M and group T (P<0.05). On D7, the wound healing rate of group H was significantly higher than group M and group T (P<0.05), and that of group T was higher than group M (P<0.05).

Comparison of wound healing time

As shown in **Table 2**, compared to group M and group T, the wound healing time of skin and muscle tissues in group H was significantly shorter (P<0.05, P<0.01), and that of group T was shorter than group M (P<0.05).

Pathological examination of PU tissues

Normal skin tissues were composed of full-layer integral structures, namely the epidermis, dermis and subcutaneous tissues, in addition to the corneum, granular, spinous layer, basal, and papillary layers. Structure of the reticular layer was clear, as well as numerous sebaceous glands, hair follicles, sweat glands, and other skin appendages, and the skin blood vessels were rich [10]. We observed that the PU model rats exhibited an empurpled leg, with a small amount of ulceration and mild exudate. HE staining confirmed that skin surface had exu-

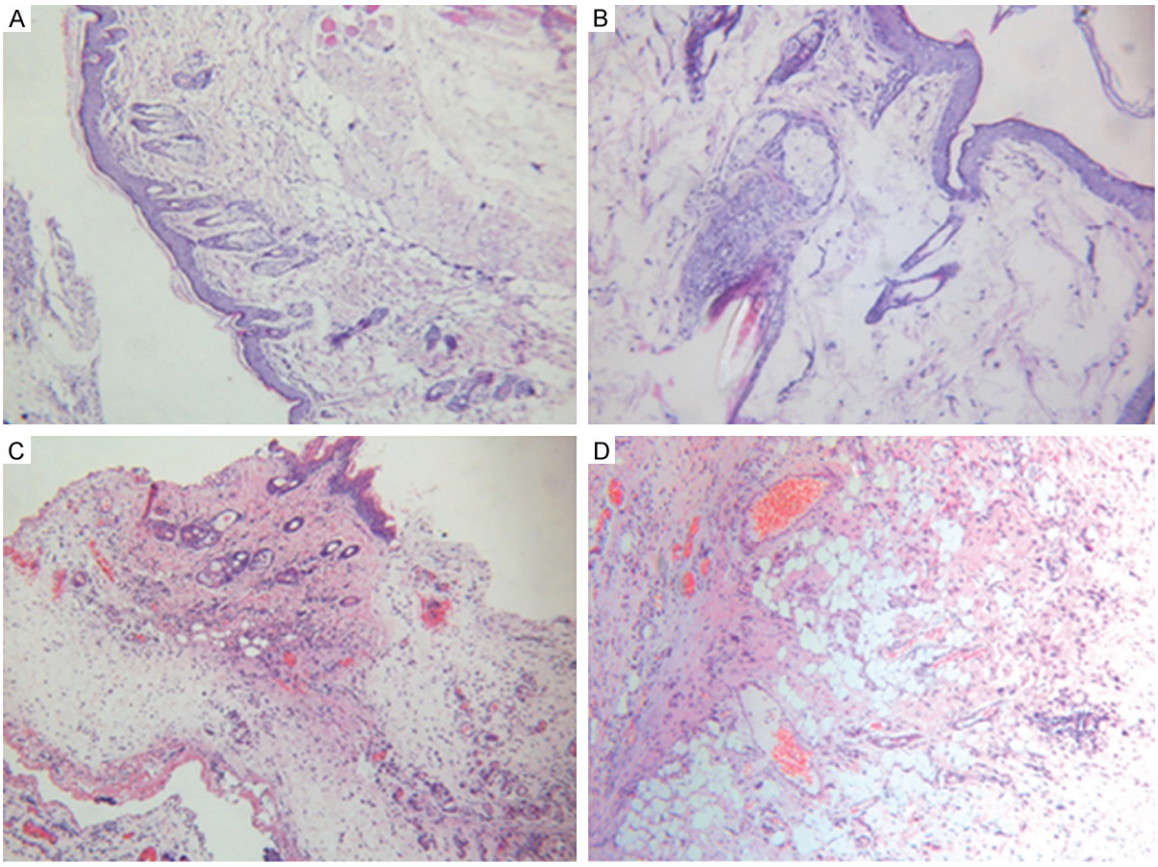

Figure 3. Pathological detection of normal skin tissues and resected necrotic tissues. Note: A: Normal skin tissues (HE×40); B: Normal skin tissues (HE×200); C: Necrotic tissues (HE×40); D: Necrotic tissues (HE×200).

dates, necrosis, fibrous proliferation, and lymphocytic infiltration (**Figure 3**).

On D1, each group exhibited dermal defects, with obvious edema in subcutaneous tissues and more inflammatory cell infiltration. Group H exhibited lighter inflammatory cell infiltration than groups T and M. Group M secreted more subcutaneous inflammatory exudate, and group H exhibited proliferation of fibrous tissues and vessels in the dermis. Compared with group M and group T, group H exhibited lighter inflammatory cell infiltration (**Figure 4**).

On D3, inflammation and edema in subcutaneous tissues of each group was eased by various degrees, group T secreted lesser inflammatory exudate than group M. Group H exhibited significantly reduced inflammatory cells than the other 2 groups, and tissue edema was significantly reduced. Group H exhibited lighter inflammatory infiltration than groups T and M, and group H exhibited significant proliferation of fibrous tissues and vessels in dermis, as well as a small amount of skin appendages (**Figure 5**).

On D7, group H exhibited significantly reduced number of inflammatory cells, and its extent of tissue edema was lower than the other two groups, indicating that the tissue defects were significantly repaired. The number of capillaries in group H was smaller than group M and group T, while that in group M was greater than group T. Collagen fibrosis proliferation, scar formation, and skin appendages were observed to increase in the dermis of group H (**Figure 6**).

Discussion

PU animal models can be divided into ischemic PU, ischemia-reperfusion PU, and bacteria-infected PU models [14, 15]. The ischemic PU model exhibited pathological changes such as hemoconcentration, characterized by an increase in blood viscosity and thrombosis,

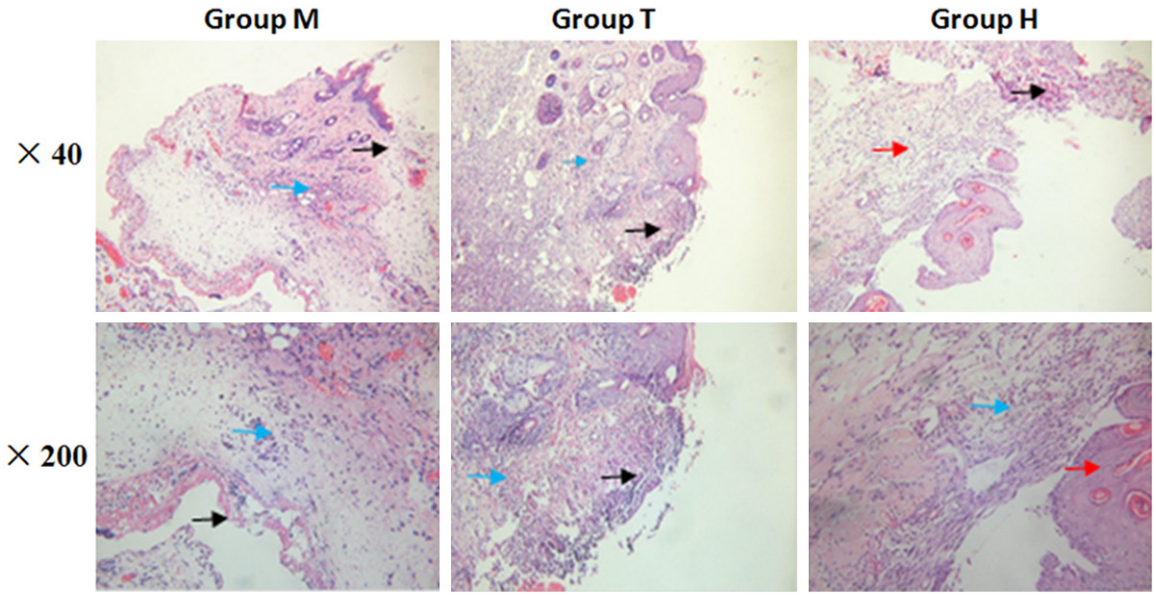

Figure 4. Comparison of HE staining of wound on D1 among the groups. Note: epidermis, inflammatory cells, blood vessels and fibrous tissues, scar tissues.

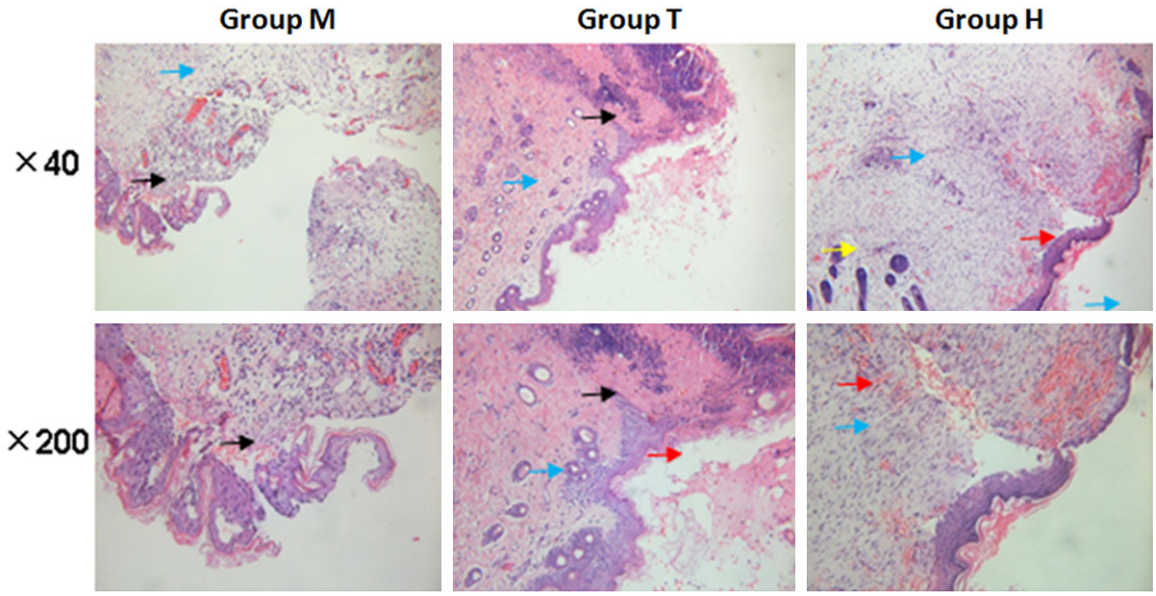

Figure 5. Comparison of HE staining of wound on D3. Note: epidermis, inflammatory cells infiltration, blood vessels and fibrous tissues, skin appendages.

which might lead to local blood circulation disorders, edema, and tissue necrosis [16]. Ischemia-reperfusion PU is caused when the body is compressed, and the capillaries are blocked, tissue ischemia-hypoxia would then induce body's compensation reactions [17]. Owing to calcium overloading, outbreak of oxygen free radicals as well as an increase in inflammatory factors further aggravated tissue- and organ-damage when blood flow was restored. Currently, the commonly observed reason for PU is ischemia-reperfusion that causes chronic skin- and muscle tissue-damage [18-20]. Presently, the magnetic compression, innerspring compression, and mechanical compression methods are normally used to

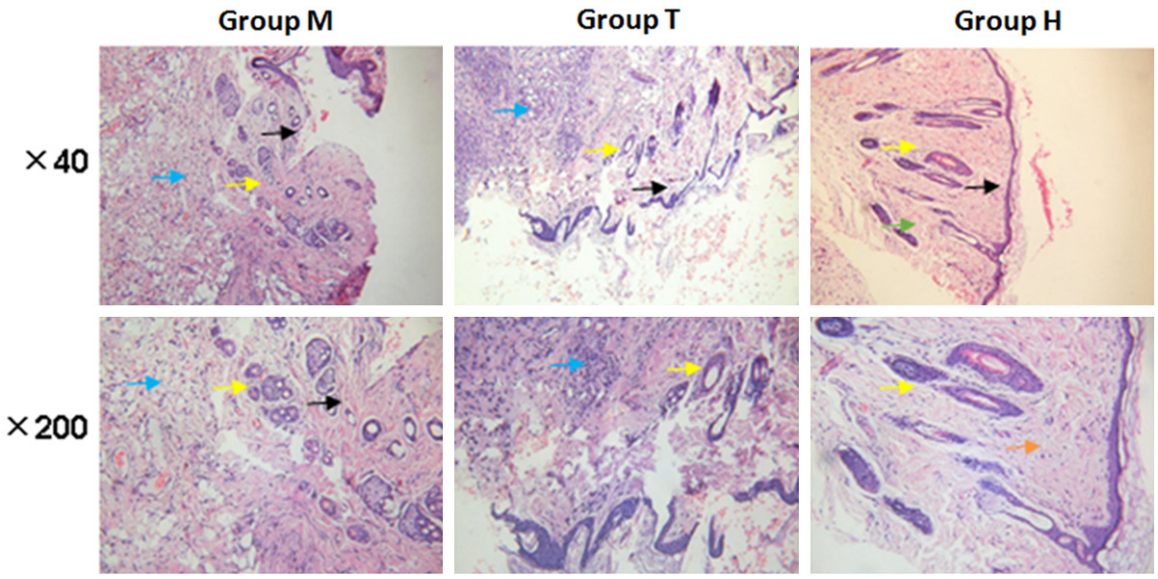

Figure 6. Comparison of HE staining of wound on D7. Note: epidermis, inflammatory cells infiltration, skin appendages, scar tissue.

generate a PU model. Because the magnetic compression method and innerspring compression method need surgical intervention, they cause bodily damages to the experimental animals; moreover, the formation mechanisms of PU cannot be elucidated using these methods. This study selected a mechanical compression method for preparation of an ischemia-reperfusion PU model of rat skin and muscle tissues. Seven days after modeling, we observed that the skin hardened and became darker. Histopathological identification confirmed our observations as stage III PU, indicating that this study successfully generated a rat PU model.

On D3, after each group received the appropriate treatment, group H exhibited significantly higher wound healing rate than the other two groups. Compared with groups M and T, group H exhibited significantly shortened wound healing time. HE staining showed that the numbers of inflammatory cells in group H at different time points were lower than group M, while the number of newborn capillary networks on D3 were higher than the other two groups, on D7, group H exhibited significantly reduced wound skin defects than the other two groups, and the numbers of capillaries under microscope were less than the other two groups, while the proliferation of a lot of collagen fibers and the formation of skin appendages could also be seen in group H.

In summary, pathological changes among different groups showed that group H exhibited the most significant improvements, indicating that hAEC transplantation could play distinct roles in the treatment stage III PU.

Disclosure of conflict of interest

None.

Address correspondence to: Dr. Zhixia Jiang, Nursing College, Zunyi Medical College, Zunyi 563000, Guizhou, China. Tel: +86 852 8608576; Fax: +86 852 8608376; E-mail: huagangchengcn@126.com

References

[1] European Pressure Ulcer Advisory Panel and National Pressure Ulcer Advisory Panel. Treatment of pressure ulcers: Quick Reference Guide. Washington DC: National Pressure Ulcer Advisory Panel, 2009.

[2] Baharestani MM and Ratliff CR. Pressure ulcers in neonates and children: an NPUAP white paper. Adv Skin Wound Care 2007; 20: 208-220.

[3] de la Garza-Rodea AS, Knaän-Shanzer S and van Bekkum DW. Pressure ulcers: description of a new model and use of mesenchymal stem cells for repair. Dermatology 2011; 223: 266-284.

[4] Barrufet MP, Vendrell E, Force L, Sauca G, Rodríguez S, Martínez E, Palomera E, Serra-Prat M, Capdevila JA, Cornudella J, Llopis A, Roble-

do MA and Vázquez C. Prevalence and risk factors for meticillin-resistant Staphylococcus aureus in an acute care hospital and long-term care facilities located in the same geographic area. Rev Esp Quimioter 2014; 27: 190-195.
[5] Yen BL, Huang HI, Chien CC, Jui HY, Ko BS, Yao M, Shun CT, Yen ML, Lee MC and Chen YC. Isolation of multipotent cells from hum n term placenta. Stem Cells 2005; 23: 3-9.
[6] Marcus AJ, Coyne TM, Rauch J, Woodbury D and Black IB. Isolation, characterization, and differentiation of stem cells derived from the rat amniotic membrane. Differentiation 2008; 76: 130-144.
[7] Girouard K, Harrison MB and VanDenKerkof E. The symptom of pain with pressure ulcers: a review of the literature. Ostomy Wound Manage 2008; 54: 30-40.
[8] Arashi M, Sugama J, Sanada H, Konya C, Okuwa M, Nakagami G, Inoue A and Tabata K. Vibration therapy accelerates healing of Stage I pressure ulcers in older adult patients. Adv Skin Wound Care 2010; 23: 321-327.
[9] Ma DH, Yao JY, Kuo MT, See LC, Lin KY, Chen SC, Chen JK, Chao AS, Wang SF and Lin KK. Generation of endostatin by matrix metalloproteinase and cathepsin from human limbocorneal epithelial cells cultivated on amniotic membrane. Invest Ophthalmol Vis Sci 2007; 8: 644-651.
[10] Manuelpillai U, Lourensz D, Vaghjiani V, Tchongue J, Lacey D, Tee JY, Murthi P, Chan J, Hodge A and Sievert W. Human amniotic epithelial cell transplantation induces markers of alternative macrophage activation and reduces established hepatic fibrosis. PLoS One 2012; 7: e38631.
[11] Yang JJ, Wang XL, Shi BW and Huang F. The angiogenic peptide vascular endothelial growth factor-basic fibroblast growth factor signaling is up-regulated in a rat pressure ulcer model. Anat Rec (Hoboken) 2013; 296: 1161-1168.
[12] Marcus AJ, Coyne TM, Black IB and Woodbury D. Fate of amnion-derived stem cells transplanted to the fetal rat brain: migration, survival and differentiation. J Cell Mol Med 2008; 12: 1256-1264.
[13] Nguyen PK, Smith AL and Reynolds KJ. A literature review of different pressure ulcer models from 1942-2005 and the development of an ideal animal model. Australas Phys Eng Sci Med 2008; 31: 223-225.
[14] Akrami H, Soheili ZS, Sadeghizadeh M, Khalooghi K, Ahmadieh H, Kanavi MR, Samiei S and Pakravesh J. Evaluation of RPE65, CRALBP, VEGF, CD68, and tyrosinase gene expression in human retinal pigment epithelial cells cultured on amniotic membrane. Biochem Genet 2011; 49: 313-322.
[15] Miki T, Lehmann T, Cai H, Stolz DB and Strom SC. Stem cell characteristics of amniotic epithelial cells. Stem Cells 2005; 23: 1549-1559.
[16] Tsutakawa S, Kobayashi D, Kusama M, Moriya T and Nakahata N. Nicotine enhances skin necrosis and expression of inflammatory mediators in a rat pressure ulcer model. Br J Dermatol 2009; 161: 1020-1027.
[17] Le Blanc K, Tammik C, Rosendahl K, Zetterberg E and Ringdén O. HLA expression and immunologic properties of differentiated and undifferentiated mesenchymal stem cells. Exp Hematol 2003; 31: 890-896.
[18] Miki T and Strom SC. Amnion-derived pluripotent/multipotent stem cells. Stem Cell Rev 2006; 2: 133-142.
[19] Neuss S, Becher E, Wöltje M, Tietze L and Jahnen-Dechent W. Functional expression of HGF and HGF receptor/c-met in adult human mesenchymal stem cells suggests a role in cell mobilization, tissue repair, and wound healing. Stem Cells 2004; 22: 405-414.
[20] Zani A, Cananzi M, Fascetti-Leon F, Lauriti G, Smith VV, Bollini S, GhiSonzoli M, D'Arrigo A, Pozzobon M, Piccoli M, Hicks A, Wells J, Siow B, Sebire NJ, Bishop C, Leon A, Atala A, Lythgoe MF, Pierro A, Eaton S and De Coppi P. Amniotic fluid stem cells improve survival and enhance repair of damaged intestine in necrotising enterocolitis via a COX-2 dependent mechanism. Gut 2014; 63: 300-309.